



## UvA-DARE (Digital Academic Repository)

### The hidden life of cosmic carbon

*Infrared fingerprint spectroscopy and fragmentation chemistry of gas-phase polycyclic aromatic hydrocarbons*

Wiersma, S.D.

#### Publication date

2021

#### License

Other

[Link to publication](#)

#### Citation for published version (APA):

Wiersma, S. D. (2021). *The hidden life of cosmic carbon: Infrared fingerprint spectroscopy and fragmentation chemistry of gas-phase polycyclic aromatic hydrocarbons*.

#### General rights

It is not permitted to download or to forward/distribute the text or part of it without the consent of the author(s) and/or copyright holder(s), other than for strictly personal, individual use, unless the work is under an open content license (like Creative Commons).

#### Disclaimer/Complaints regulations

If you believe that digital publication of certain material infringes any of your rights or (privacy) interests, please let the Library know, stating your reasons. In case of a legitimate complaint, the Library will make the material inaccessible and/or remove it from the website. Please Ask the Library: <https://uba.uva.nl/en/contact>, or a letter to: Library of the University of Amsterdam, Secretariat, Singel 425, 1012 WP Amsterdam, The Netherlands. You will be contacted as soon as possible.

## Appendix A

---

### Appendices to Chapter 4

---

#### A.1 Anthracene

##### A.1.1 Anthracene cation mass spectrum

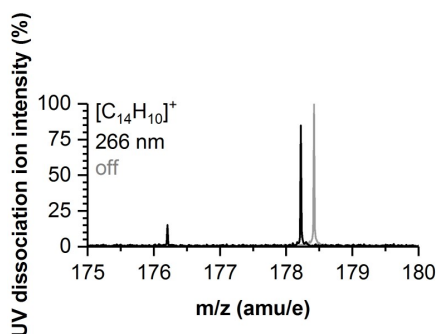


FIGURE A.1: Fragmentation mass spectrum of the anthracene cation  $C_{14}H_{10}^+$ . The black trace was recorded after exposure to 1 mJ pulses at 10 Hz of a 266 nm (4th harmonic of a Nd:YAG laser) for 3 s, while the gray trace was recorded with the laser off and was given an offset of 0.2 amu for legibility.

Figure A.1 shows fragmentation mass spectra for the radical cation  $C_{14}H_{10}^+$  at  $m/z = 178$  (gray). After UV irradiation (black), the fragmentation mass spectrum shows one fragment at  $m/z = 176$ , depicting the loss of two H atoms as the only dissociation process from the radical cation, which was also observed by Ekern *et al.* [205].

A quantitative interpretation of mass spectra exhibiting sequential H-loss could be complicated by the presence of naturally abundant  $^{13}C$  isotopologs of the PAH under investigation, amounting to 15.3 % for a molecule with 14 carbons. To ensure the isotopic purity, the mass spectra were made as clean as possible prior to isolation, that is, minimizing the intensity of the cations in the case of protonation, and optimizing deuteronation versus protonation for the deuterated anthracene. Using unisolated mass spectra, it is possible to make accurate estimates of the isotopic contamination in the precursor peaks

for each spectrum. Knowing that the cation only loses two hydrogen atoms, we can distinguish contributions of the protonated and deuterated isomers from the contributions of the radical cationic  $^{13}\text{C}$  isomers.

### A.1.2 Anthracene band positions

Table A.1 lists all of the measured band positions of protonated anthracene featured in Fig. 4.1g–i, and compares them with the theoretical band positions of the three different position isomers as calculated using DFT.

Table A.2 lists those measured and calculated for deuterated anthracene given in Fig. 4.1j–l. Interestingly, the only band not predicted by the 9-isomer is precisely the experimental band at  $1360\text{ cm}^{-1}$ . Suitable modes are predicted at  $1355\text{ cm}^{-1}$  for the 1-isomer (k) and at  $1363$  for the 2-isomer (l). However, the predicted features of the 1- and 2-isomers around  $900\text{ cm}^{-1}$  are not present in the experiment. Overall, the features are consistent with the 9-isomer.

Table A.3 lists all measured and calculated for protonated, perdeuterated anthracene given in Fig. 4.1m–o. Only calculated frequencies that exhibit enough intensity to allow for comparison with the experimental features are listed.

### A.1.3 Theoretical spectra for additional anthracene isomers

Figure A.2 displays the six different isotopic isomers that can be formed by a  $[\text{D}-\text{C}_{14}\text{H}_{10}]^+$  with the aliphatic group at the 9-position. These spectra mostly differ in terms of intensity ratios. The only spectrum showing significant changes in band position, is the one where the D is at the 5 site, opposite the C–HH group, which is the most symmetric configuration. This increased symmetry leads to improved resonant enhancement of the in-plane C–H bending vibrations, which significantly changes the shape of the spectrum. However, this theoretical spectrum is clearly not in agreement with the experimental spectrum.

## A.2 Phenanthrene

### A.2.1 Band positions for phenanthrene

Table A.4 lists all of the measured bands visible in Fig. 4.4b–f, and compares them with the calculated band positions of the five different position isomers.

## A.2. Phenanthrene

TABLE A.1: Band positions in  $\text{cm}^{-1}$  of the experimental spectrum of protonated anthracene  $[\text{H}-\text{C}_{14}\text{H}_{10}]^+$  and the most intense modes of the unconvoluted, theoretical spectra, capped off at 10 km/mol. A scaling factor of 0.9662 has been applied to the calculated spectrum to correct for anharmonicity. The experimental IR intensities are normalized to the highest intensity, while the theoretical IR intensities are the absolute cross sections in km/mol.

$[\text{H}-\text{C}_{14}\text{H}_{10}]^+$							
experiment		9-isomer		1-isomer		2-isomer	
$\bar{\nu}$ ( $\text{cm}^{-1}$ )	I (a.u.)	$\bar{\nu}$ ( $\text{cm}^{-1}$ )	I (km/mol)	$\bar{\nu}$ ( $\text{cm}^{-1}$ )	I (km/mol)	$\bar{\nu}$ ( $\text{cm}^{-1}$ )	I (km/mol)
759	0.11	755	84	743	41	741	38
						873	34
						886	11
						888	16
						900	15
						911	11
						944	20
						1005	11
						1163	25
						1166	15
1146	0.49	1146	88	1047	15	1005	11
						1166	15
						1166	15
1185	0.30	1191	63	1177	88	1181	68
						1223	70
						1221	28
						1257	12
1319	0.61	1276	20	1257	12	1261	13
						1290	74
						1309	113
						1312	220
						1324	139
						1337	18
						1335	35
						1333	26
						1355	43
						1355	128
1445	1.00	1409	65	1376	22	1364	163
						1438	168
						1432	324
						1441	25
						1441	66
						1466	25
1505	0.84	1476	18	1492	404	1506	32
						1501	305
						1521	85
						1523	56
1581	0.83	1535	11	1521	85	1568	99
						1539	35
						1555	101
						1578	429
						1590	14
		1592	21	1602	228	1592	443
						1611	103
						1611	103

TABLE A.2: Band positions in  $\text{cm}^{-1}$  of the experimental spectrum of deuterated anthracene  $[\text{D}-\text{C}_{14}\text{H}_{10}]^+$  and the most intense modes of the unconvoluted, theoretical spectra, capped off at 10 km/mol. A scaling factor of 0.9662 has been applied to the calculated spectrum to correct for anharmonicity. The experimental IR intensities are normalized to the highest intensity, while the theoretical IR intensities are the absolute cross sections in km/mol.

$[\text{D}-\text{C}_{14}\text{H}_{10}]^+$									
experiment		9-isomer		1-isomer		2-isomer			
$\bar{\nu}$ ( $\text{cm}^{-1}$ )	I (a.u.)	$\bar{\nu}$ ( $\text{cm}^{-1}$ )	I (km/mol)	$\bar{\nu}$ ( $\text{cm}^{-1}$ )	I (km/mol)	$\bar{\nu}$ ( $\text{cm}^{-1}$ )	I (km/mol)		
758	0.07	755	86	743	44	737	13		
						742	26		
1146	0.42	1150	81	811	14	869	29		
						828	10	888	20
						896	35	913	28
						1048	17	950	14
						1159	50	1142	33
1191	0.24	1158	12	1177	95	1152	137		
						1167	19	1155	46
						1188	66	1183	26
1315	0.61	1201	25	1223	54	1220	29		
						1276	20	1261	12
						1308	178	1307	15
1360	0.27	1333	54	1319	19				
						1355	168	1363	194
						1374	25	1380	48
1439	1.00	1406	55	1403	13				
						1424	6		
						1432	334	1441	65
								1466	27
1499	0.85	1474	25	1490	434	1505	42		
						1520	81	1523	61
						1534	13	1538	35
1569	1.00	1538	35	1554	92	1567	93		
						1577	429	1592	473
						1592	21	1609	95
				1602	237				

TABLE A.3: Band positions in  $\text{cm}^{-1}$  of the experimental spectrum of protonated, perdeuterated anthracene  $[\text{H}-\text{C}_{14}\text{D}_{10}]^+$  and the most intense modes of the unconvoluted, theoretical spectra, capped off at 10 km/mol. A scaling factor of 0.9662 has been applied to the calculated spectrum to correct for anharmonicity. The experimental IR intensities are normalized to the highest intensity, while the theoretical IR intensities are the absolute cross sections in km/mol.

$[\text{H}-\text{C}_{14}\text{D}_{10}]^+$							
experiment		9-isomer		1-isomer		2-isomer	
$\bar{\nu}$ ( $\text{cm}^{-1}$ )	I (a.u.)	$\bar{\nu}$ ( $\text{cm}^{-1}$ )	I (km/mol)	$\bar{\nu}$ ( $\text{cm}^{-1}$ )	I (km/mol)	$\bar{\nu}$ ( $\text{cm}^{-1}$ )	I (km/mol)
		938	29	932	11		
		1139	13			1152	134
		1197	13	1179	74		
		1206	31				
				1227	14	1233	14
		1277	67			1289	24
		1311	70				
1321	0.13	1324	13	1327	112	1337	291
		1349	28	1334	39	1349	33
1380	0.21	1371	110	1402	263	1391	9
		1389	19	1403	46	1410	43
1450	1	1451	451	1452	552	1473	16
		1494	73	1486	169	1488	120
		1499	27	1506	74	1532	11
1540	0.79	1540	555			1560	524
		1559	14	1575	273	1577	162

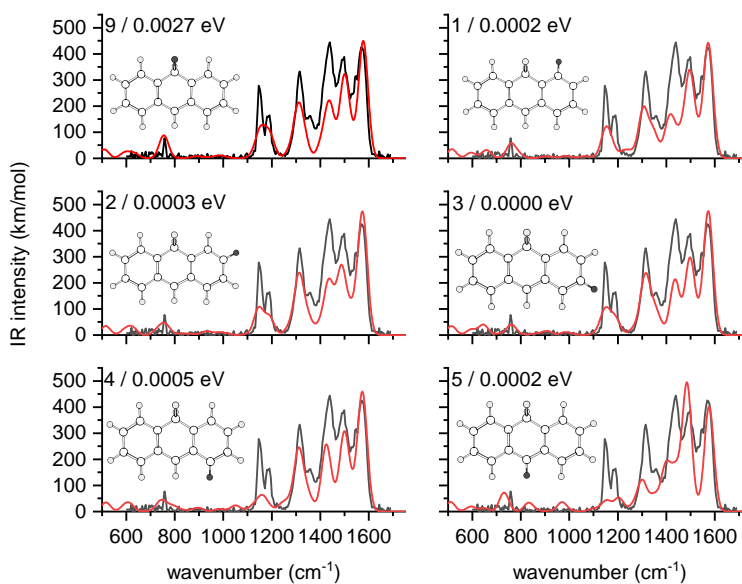


FIGURE A.2: Calculations for the six scrambled isomers of the 9-isomer of deuterated anthracene (red) compared to the FELIX IRMPD spectrum of [D-C<sub>14</sub>H<sub>10</sub>]<sup>+</sup> (black). The shifting D atom is marked in black on the molecule, and the label in the upper right corner of each panel indicates its position. The energy of each of these isomers is listed in eV with respect to the global minimum.

TABLE A.4: Band positions in  $\text{cm}^{-1}$  of the experimental spectrum of protonated, perdeuterated phenanthrene  $[\text{H}-\text{C}_{14}\text{D}_{10}]^+$  and the most intense modes of the unconvoluted, theoretical spectra, capped off at 10  $\text{km/mol}$ . A scaling factor of 0.9662 has been applied to the calculated spectrum to correct for anharmonicity. The experimental IR intensities are normalized to the highest intensity, while the theoretical IR intensities are the absolute cross sections in  $\text{km/mol}$ .

experiment		$\text{H}^+\text{C}_{14}\text{D}_{10}$											
$\tilde{\nu}$ ( $\text{cm}^{-1}$ )	I (a.u.)	9-isomer		1-isomer		3-isomer		4-isomer		2-isomer			
		$\tilde{\nu}$ ( $\text{cm}^{-1}$ )	I ( $\text{km/mol}$ )	$\tilde{\nu}$ ( $\text{cm}^{-1}$ )	I ( $\text{km/mol}$ )	$\tilde{\nu}$ ( $\text{cm}^{-1}$ )	I ( $\text{km/mol}$ )	$\tilde{\nu}$ ( $\text{cm}^{-1}$ )	I ( $\text{km/mol}$ )	$\tilde{\nu}$ ( $\text{cm}^{-1}$ )	I ( $\text{km/mol}$ )		
		1080	24			1108	22						
		1119	15			1145	128						
		1152	74	1153	81	1303	60	1154	29	1137	120		
				1168	23	1308	103						
		1298	44	1314	394	1352	125	1323	48	1314	83		
1353	1	1351	284	1317	22	1365	55	1332	187	1345	31		
		1367	169	1332	165			1387	46	1382	182		
		1387	23					1398	262				
				1456	323	1435	125	1451	284	1402	39		
1463	0.75	1450	99			1452	277			1465	48		
										1496	65		
						1520	238	1483	24	1532	232		
		1551	44	1510	170	1541	29	1517	29	1558	100		
1565	0.59	1560	287	1556	54	1579	115	1566	134	1567	140		